Rev. Roum. Sci. Techn.– Électrotechn. et Énerg.
Vol. **62**, *2*, pp. 185–191, Bucarest, 2017

STUDY OF THE INPUT CURRENT HARMONIC DISTORTION OF VOLTAGE-SOURCE ACTIVE RECTIFIERS

VACLAV KUS, TEREZA JOSEFOVA

Key words: Harmonic analysis, Power quality, Pulse width modulation (PWM), Total harmonic distortion, Voltage-source active rectifier.

This paper presents the description of the current distortion produced to the grid by voltage-source active rectifiers switched by PWM. In recent years, high demands are placed on the development of the power electronics such as high performances, high switching frequencies, high efficiency, etc. Therefore the aim of the paper is the cognition of the influence combination of switching frequencies and dead time durations on harmonics orders and values in an input current spectrum. The paper summarizes the parameters influences on the calculations of current total harmonic distortion (THD_I) and presents interesting results of two THD_I definitions. If the THD_I is calculated up to the frequency which is higher than the switching frequency, the result will be different from the result which is obtained according to IEC standard. Therefore, this paper proves that total harmonic distortion has to be calculated up to the harmonics orders that are higher than the switching frequency of the converter.

1. INTRODUCTION

In recent years, the development of power electronics grows up. The high demands are placed on the high performances, high efficiencies, low produced harmonic distortion and the related high switching frequencies. Therefore, this paper is aimed at the current harmonics calculations method of the current drawn from the grid by voltage-source active rectifiers. The introduction of the article shows that the harmonic analysis of the voltage produced by voltage-source inverters can be used for the derivation of voltage-source active rectifiers input current harmonics orders and values.

The first publications which deal with the description of a pulse width modulation appear after year 1970. They describe the influences of inverters on motors. Authors of the articles [1, 2] who were motivated by the paper [3] focus on the analytical description of a pulse width modulation using Fourier series.

For example, the theory of a pulse width modulation was further elaborated by J. Hamman and F.S. Van der Merwe in the publication [4] which mathematically describes a two-level PWM signal that is expressed as the equation (1).

$$F(t)=\frac{MV}{2}\cos(\omega_F t)+ \\ +\frac{2V}{\pi}\sum_{m=1}^{\infty}J_0\left(mM\frac{\pi}{2}\right)\sin\left(m\frac{\pi}{2}\right)\cos(m\omega_C t)+ \\ +\frac{2V}{\pi}\sum_{m=1}^{\infty}\sum_{n=\pm1}^{\pm\infty}\frac{J_n\left(mM\frac{\pi}{2}\right)}{m}\sin\left[\left(m+n\frac{\pi}{2}\right)\right]\cos(m\omega_C+n\omega_F t), \quad (1)$$

where ω_F is the frequency of a sinus signal, ω_C is the frequency of a triangle signal, M is the modulation signal, V is the dc supply voltage value of an inverter, J_0 and J_n are Bessel functions of the first order and n and m are positive nonzero integer. The equation (1) is composed of three components. The first component indicates the amplitude of the first harmonic; the second component presents the harmonics amplitudes that have frequencies equal to the frequency of a triangle signal and its integer multiples; the third component describes information about harmonics amplitudes of sidebands around integer multiples of the triangle signal frequency.

The most detailed publication that deals with the analysis of pulse width modulation is the book [5]. It describes variants of a PWM; for example, PWM with the third harmonic injection, PWM that eliminates harmonics, etc.

The paper [6] shows the mathematical analysis and comparative study of carrier-frequency modulation techniques for conducted electromagnetic interference suppression in voltage-source inverters. The ideal voltage signal u_{A0i} produced by a pulse width modulation is expressed in the equation (2) and it is shown in Figs. 1 and 2; transistors are assumed to be ideal.

$$u_{A0i}=\sum_{h=-\infty}^{\infty}c_h\left\{\begin{array}{l}J_0(hm_F)\mathrm{e}^{\mathrm{j}h2\pi f_{SW}t}+\\ +\sum_{k=1}^{\infty}J_n(hm_F)\left[\begin{array}{l}\mathrm{e}^{\mathrm{j}2\pi(hf_{SW}+kf_m)t}+\\ +(-1)^k\mathrm{e}^{\mathrm{j}2\pi(hf_{SW}-kf_m)t}\end{array}\right]\end{array}\right\}. \quad (2)$$

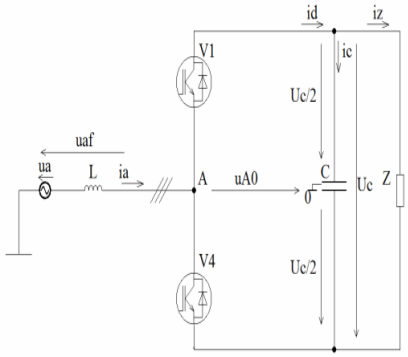

Fig. 1 – Detailed representation of a voltage-source active rectifier.

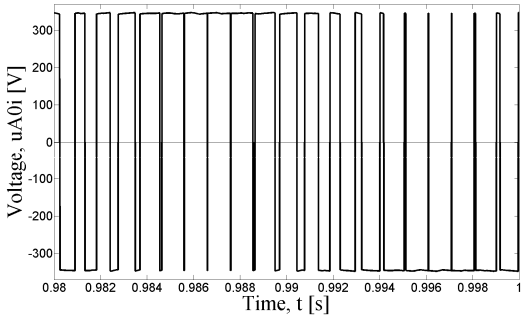

Fig. 2 – Ideal voltage waveform u_{A0i}.

University of West Bohemia, Department of Electromechanics and Power Electronics, Univerzitni 24, 306 14 Plzen, Czech Republic, Email: kus@kev.zcu.cz, terkajos@kev.zcu.cz.

In modulation ideal voltage signal spectrum is composed by the sidebands of harmonics around the switching frequency f_{sw} (the frequency of a triangle signal) and its integer multiples. Around each h-multiple there are sidebands of the harmonics. Spacing is equal to k-multiples of the modulation frequency f_m (the frequency of a control signal).

All these publications deal with the ideal pulse width modulation; it means that semiconductor elements are switched immediately. In fact, the transistors in a one branch of voltage-source active rectifiers cannot be switched on immediately after switch-off; minimum time (dead time) has to be kept between semiconductor elements in a branch.

The first paper [7] which deals with the influence of the dead times presents the analysis of the pulse width modulation with the dead times. This paper compares the waveforms of the PWM with and without the dead times. The difference of these two curves is a waveform of pulses that have the same length. The dead times influence the characteristics harmonics satisfying the equation (3)

$$h = kp \pm 1, \tag{3}$$

where h is the harmonic order, k is the integer multiple, p is the pulsation of converters.

More sophisticated methods of dead times descriptions are showed in [8–10]. The authors of the newest papers replace the waveform of the dead time pulses by Dirichlet pulses.

The importance of the power quality monitoring is described in [11]. The methods that are used for the eliminations of harmonics currents are presented in [12]. The publication [13] shows the possibility of the THD_I minimization by the connections of active filters which are costly and complex solutions and have ratings comparable to the load rating presented in [14].

Further investigation directions of input current harmonics of voltage-source active rectifiers are control methods eliminating current harmonics or increasing the robustness of the systems. The article [15] presents the repetitive controller which is used for dead time compensation. The paper [16] deals with sliding mode virtual flux oriented control which leads to improvement of the robustness against load changes and supply variations.

The authors of this paper deal with the description of the current harmonics drawn from the grid by voltage source active rectifiers which is commonly used in industry. The aim is the cognition of parameters influences on harmonics orders and values in the input current spectrum; the effects of the pulse width modulation and dead times are presented. In the end, the summary of these parameters influences is illustrated by the total harmonic distortion of the input current (THD_{Ia}). If the switching frequency is higher than 2.5 kHz, the level of THD_{Ia} calculation is important. Therefore two definitions of the total harmonic distortion of the input current are showed in three-dimensional graphs. In the end, the paper proves the importance of the calculation of the THD_{Ia} up to the harmonics orders that are higher than switching frequencies of the converters.

2. PRINCIPLE OF THE CURRENT HARMONICS CALCULATION

The principle of voltage-source inverters and harmonic analysis of the PWM is presented in the above-mentioned introduction. The principle of voltage-source active rectifiers and current harmonic analyzes are shown in [17–19]. The current waveform i_a drawn from the grid by voltage-source active rectifiers can be described according to the equivalent circuit in Fig. 3. This is an approach which uses the harmonic analysis knowledge of voltage-source inverters. The "modified one over h rule" that is presented in the [20] and applied for the classic rectifiers cannot be used due to the sinusoidal character of the current drawn from the grid by voltage-source active rectifiers.

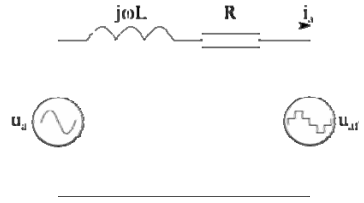

Fig. 3 – Schematic representation of a voltage-source active rectifier.

The voltage source u_a which is in the left side of Fig. 3 is considered to be ideal. The real distortion of the voltage source is transmitted to the distortion of the input current i_a; this phenomenon is not included in this paper. The input reactance (R, L) contains the reactance of the grid and the necessary elements for proper function of a converter. The ideal input voltage of the voltage-source active rectifier u_{afi} which is composed of the voltages u_{A0i}, u_{B0i} and u_{C0i} in Fig. 2 (u_{afi}=1/3($2u_{A0i} - u_{B0i} - u_{C0i}$)) is in the right side of Fig. 3. The harmonic analysis of the ideal voltage u_{afi} is discussed in the above-mentioned part. In accordance with these calculations, the first ideal input current harmonic $I_{ami(h)}$ is expressed in the equation (4) according to a phasor diagram that can be drawn for the equivalent circuit.

$$I_{ami(1)} = \frac{2RU_{a(1)} + \sqrt{4U_{afi(1)}^2\left(R^2 + \omega_1^2L^2 - \right) \\ -4\omega_1^2L^2U_{a(1)}^2}}{2\left(R^2 + \omega_1^2L^2\right)} \text{ [A]}, \tag{4}$$

where ω_1 is the grid frequency, U_a is the supply voltage and U_{af} is the converter input voltage shown in Figs. 2 and 3.

Harmonics of ideal input current $I_{ai(h)}$ are expressed in the equation (5).

$$I_{ai(h)} = \frac{U_{afi(h)}}{\sqrt{R^2 + \left(h\omega_1L\right)^2}} \text{ [A]}. \tag{5}$$

This method based on the equivalent circuit is advantageous because the non-ideal voltage source properties can be respected. If the voltage source waveform does not consist only of the first harmonic, the equation (5) is rewritten as the equation (6).

$$I_{ai(h)} = \frac{\sqrt{U_{afi(h)} + U_{a(h)}^2}}{\sqrt{R^2 + \left(h\omega_1L\right)^2}} \text{ [A]}, \tag{6}$$

where $U_{a(h)}$ is the h^{th} harmonic of the voltage source.

3. ASPECTS OF THE CURRENT HARMONICS CALCULATIONS

The above-mentioned equations calculate the harmonic orders and values that appear in the input current spectrum. The next parts of the paper present the properties of the converter that are affected by the mentioned parameters. First, the harmonic analyzes of the input current are showed if semiconductor elements are considered ideal; it means semiconductors elements are switched immediately. In accordance with the equivalent circuit and the equation (2), the harmonics in the spectrum of the current drawn from the grid appear around the switching frequency and its multiples. The switching frequency can also be non-integer multiple of the grid frequency, therefore the second part deals with the analysis of this case. The grid frequency is 50 Hz (f = 50 Hz).

The last part of this section considers a non-ideal PWM, it means that minimum time delay has to be inserted between the switching of two semiconductor elements in one branch. Therefore, this part shows analyzes of the dead time duration effect.

3.1. IDEAL VOLTAGE-SOURCE ACTIVE RECTIFIER (WITHOUT THE DEAD TIMES)

3.1.1. Switching frequency is the integer multiple of the grid frequency

Figure 4 shows the waveform of the current drawn from the grid by the voltage-source active rectifier. The current is little distorted and follows a sinewave. Figure 5 presents the harmonics analysis of the current drawn from the grid in Fig. 4, if the pulse width modulation is ideal, it means that the dead time duration is set to 0 s. The harmonic analysis is performed up to the 50th harmonic with respect to IEC standard [21]. Current harmonics appear around the switching frequency f_{SW} that is set to 2 kHz; the current spectrum satisfies the equation (2). Characteristics harmonics satisfying the equation (3) are negligible, because the pulse width modulation is ideal.

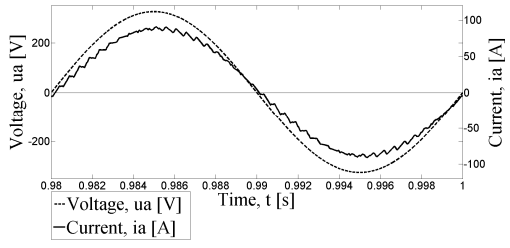

Fig. 4 – Waveforms of the input current i_a and supply voltage u_a, switching frequency f_{SW} is set to 2 kHz.

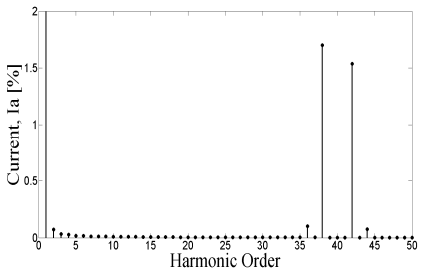

Fig. 5 – Harmonic analysis of the input current i_a in the Fig. 4, reduced y-scale.

3.1.2. Random switching freqeuncy

This part of the paper compares the harmonic analyzes of the input currents if the switching frequency is integer multiples of the grid frequency and if the switching frequency is random. Figure 6 shows the input current waveforms if the switching frequency is set to 800 Hz and 825 Hz and the pulse width modulation is ideal. It is obvious that the current waveforms are not different. Figure 7 compares the harmonic analyzes of the currents in Fig. 6. The harmonic analyzes are performed up to the 50th harmonic according to IEC standard [21]. For better illustration of the random switching influence, the input current spectra are continuous. Results confirm that the current harmonics do not increase even if the switching frequency is not integer multiple of the grid frequency. The current harmonics appear around the switching frequency.

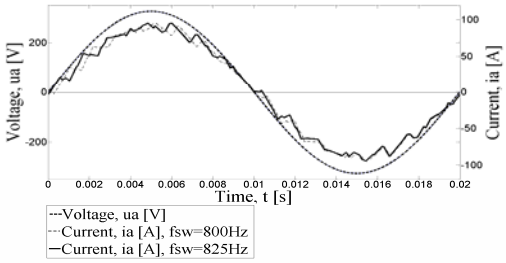

Fig. 6 – Waveforms of the input currents i_a and supply voltage u_a, the switching frequencies f_{SW} are set to 800 Hz and 825 Hz.

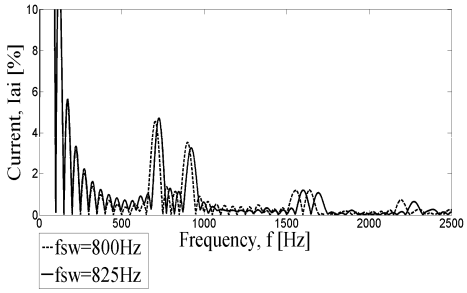

Fig. 7 – Harmonic analysis of the input current i_a in the Fig. 6, reduced y-scale.

Figure 8 presents a comparison of the harmonic analyzes of the input currents if the switching frequencies are random. The input current spectra are continuous for understanding the random switching effects. The current harmonics appear around the switching frequency and its integer multiples. The absolute values of the harmonics decrease with the increasing switching frequency.

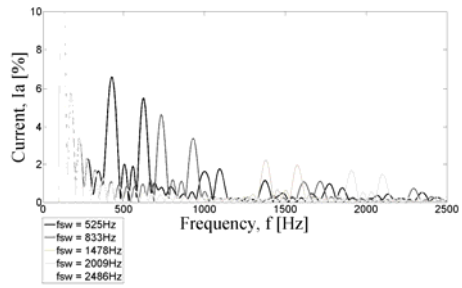

Fig. 8 – Comparison of the current harmonic analyzes, reduced y-scale, switching frequencies f_{SW} are set to random values (f_{sw} = 525 Hz, f_{sw} = 833 Hz, f_{sw} = 1478 Hz, f_{sw} = 2009 Hz, f_{sw} = 2486 Hz).

3.2. VOLTAGE-SOURCE ACTIVE RECTIFIER WITH THE DEAD TIMES

The publications [22–26] present the analytical description of the dead times principle and mathematical analysis is shown in paper [27]. The dead times affect the characteristics harmonics according to the equation (3).

Figure 9 shows the dead times pulses that are obtained by differential of ideal PWM voltage u_{A0i} and PWM voltage with dead times u_{A0} with regard to the equation (7). The dashed rectangle line in Fig. 9 is received by mean values connection of the dead times pulses which have the same duration; the height m of the rectangle is expressed in the equation (8). Therefore the dead times influence the characteristics harmonics according to the equation (3). Figure 10 illustrates the spectrum of the dead times pulses.

$$u_{A0_{DT}} = u_{A0_i} - u_{A0}\,, \tag{7}$$

$$m = f_{SW} t_D U_C\,. \tag{8}$$

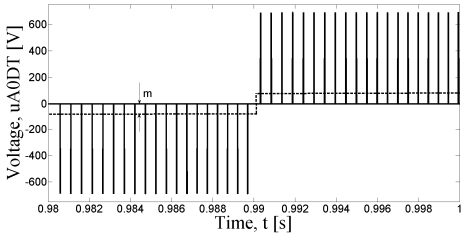

Fig. 9 – Waveform of the dead times pulses u_{A0DT}.

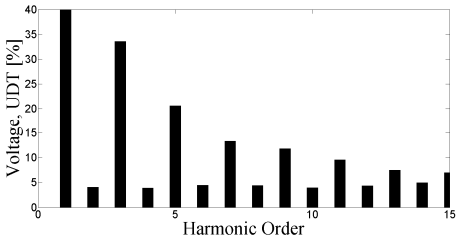

Fig. 10 – Harmonic analysis of the dead times pulses in Fig. 9.

According to the equivalent circuit in Fig. 3, the current harmonics $I_{a(h)}$ are calculated in the equation (9). With regard to equation (4), the ideal input voltage of the voltage-source active rectifier u_{afi} is replaced by the sum of the ideal input voltage of the voltage-source active rectifier u_{afi} and the waveform of the dead times pulses u_{afDT} which consists of u_{A0DT}, u_{B0DT} and u_{C0DT} (u_{afDT}=1/3(2u_{A0DT} − u_{B0DT} − u_{CDTi})).

$$I_{a(h)} = \frac{U_{afi(h)} - U_{afDT}}{\sqrt{R^2 + \left(h\omega_1 L\right)^2}}\ \text{[A]}. \tag{9}$$

Figure 11 presents the input current waveform if the switching frequency is set to 2 kHz and the dead time duration is set to 6 µs. Figure 12 shows the harmonic analysis of the input current in Fig. 11. The harmonic analysis is performed up to the 200th harmonic due to comparison with Fig. 5 and discussing the definition of total harmonic distortion in the next section. It is obvious that the current harmonics appear around the switching frequency and its multiples, the dead times cost characteristic harmonics with regard to the equation (3), mainly the 5th harmonic.

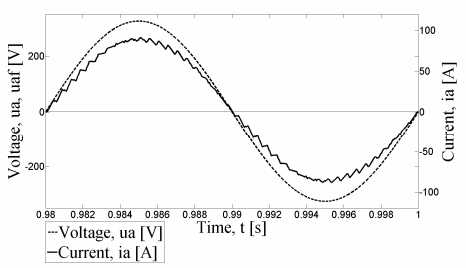

Fig. 11 – Waveforms of the input current i_a and supply voltage u_a, switching frequency f_{SW} is set to 2 kHz, dead time t_d is set to 6 µs.

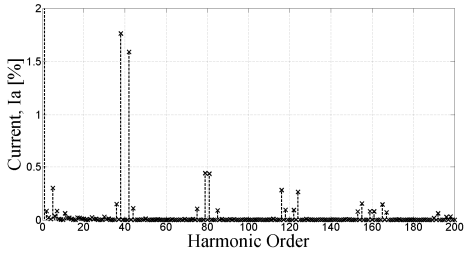

Fig. 12 – Harmonic analysis of the input current i_a in Fig. 11, reduced y-scale.

3.3. COMPARISON OF THE VOLTAGE-SOURCE ACTIVE RECTIFIERS WITH THE DEAD TIMES AND WITHOUT THE DEAD TIMES

This part compares the harmonic analyzes if the PWM is ideal and if the dead times are considered. The switching frequencies are set to three values and the dead time duration is set to 6 µs. Figure 13 shows the comparison of the input currents harmonic analyzes if the switching frequency is set to 1 kHz. Figure 13 discusses that the dead times do not influence the current distortion, because the switching frequency is low.

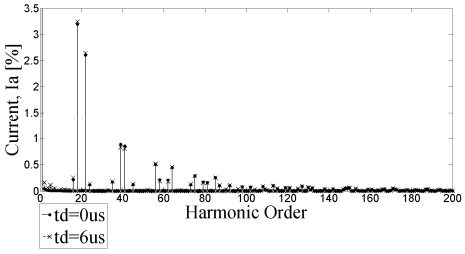

Fig. 13 – Comparison of the input currents harmonics analyzes, reduced y-scale, switching frequency f_{SW} is set to 1 kHz, dead times t_d are set to 0 s and 6 µs.

Figure 14 presents the harmonic analyzes comparison if the switching frequency is set to 3 kHz. It is obvious that the dead times influence the characteristics harmonics according to the equation (3), mainly the 5th harmonic.

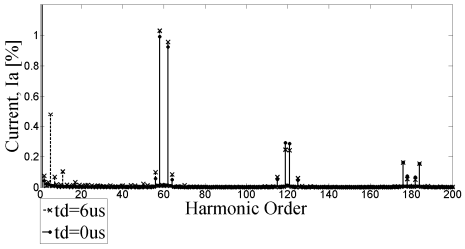

Fig. 14 – Comparison of the input currents harmonics analyzes, reduced y-scale, switching frequency f_{SW} is set to 3 kHz, dead times t_d are set to 0 s and 6 µs.

Figure 15 compares harmonic analyzes of the input currents if the switching frequency is set to 7 kHz. The switching frequency is high, therefore the dead times have main effect on the input current distortion. It is obvious that the dead times influence the characteristics harmonics according to the equation (3).

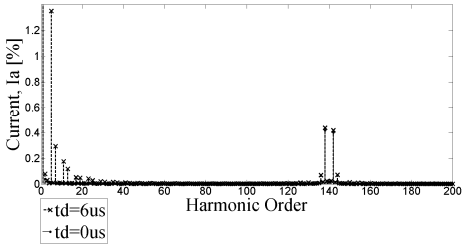

Fig. 15 – Comparison of the input currents harmonics analyzes, reduced y-scale, switching frequency f_{SW} is set to 7 kHz, dead times t_d are set to 0 s and 6 μs.

4. CALCULATIONS OF THE TOTAL HARMONIC DISTORTION OF THE CURRENT

The total harmonic distortion of the current THD_{Ia} is defined as the ratio of the current harmonics distortion to the fundamental current harmonic (in contrast with THF that is defined as the ratio of the current harmonics distortion to the rms value of the current). THD_{Ia} is the main indicator of power converters interference and it is defined in the equation (10).

$$\mathrm{THD}_{Ia} = \sqrt{\sum_{h=2}^{H}\left(\frac{I_{a(h)}}{I_{a(1)}}\right)^2} = \frac{\sqrt{\sum_{h=2}^{H} I_{a(h)}^2}}{I_{a(1)}}, \quad (10)$$

where h is the harmonic order, H is the calculation limit of the THD_{Ia} equation, I_h is the rms value of the h^{th} harmonic and I_1 is the rms value of the first harmonic.

IEC standard [21] recommends to calculate the THD up to the 50th harmonic (H = 50). The standard does not include the conditions of the harmonics source neither the high frequencies that are produced. This definition is used even if the switching frequency is higher than 2.5 kHz; it means that the harmonics orders higher than 50th harmonic are not included in the input current spectrum. This part of the paper deals with two formulations of the THD_{Ia}. First, the THD_{Ia} is calculated up to the 50th harmonic (H = 50). Second, the THD_{Ia} is performed up to the 200th harmonic (H = 200); it means that the switching frequency higher than 2.5 kHz is included in the THD_{Ia} calculation.

4.1. CALCULATION OF THE THD_{IA} ACCORDING TO THE IEC STANDARD (H = 50)

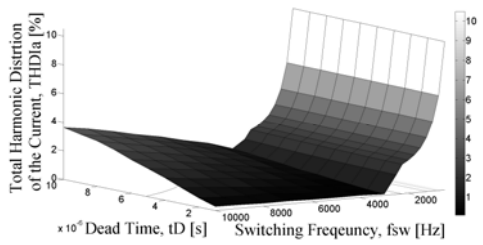

Fig. 16 – THD_{Ia} calculated up to the 50th harmonic according to the IEC standard.

From Fig. 16, it is obvious that the negative effect of the converter on the grid decreases with the increasing switching frequency. It is evident that the influence of the dead times increases with the increasing switching frequency.

4.2. CALCULATION OF THE THD_{Ia} UP TO 100 kHZ (H = 200)

This part presents the change of the THD_{Ia} curve, if the standard is not met; the THD_{Ia} is calculated up to a high harmonic order. The THD_{Ia} is performed up to the 200th harmonic with regard to possible switching frequency of converters. Figure 17 shows the three-dimensional graph of the influence of the THD_{Ia} on the switching frequency and dead time duration. The same above conclusion can be written for this formulation of the THD_{Ia}. The frequency of 10 kHz is chosen with regard to the possible switching frequencies of voltage-source active rectifiers; the current harmonics higher than 2.5 kHz appear in the spectrum of the drawn current. The aim of this definition of the THD_{Ia} (H = 200) is to discuss the influence of the harmonics order that are higher than the 50th harmonic.

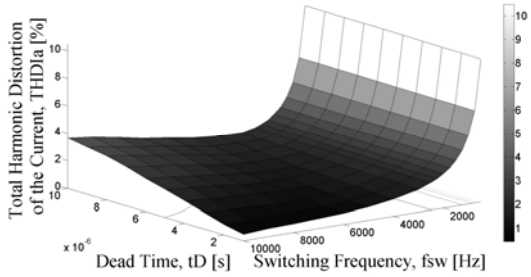

Fig. 17 – THD_{Ia} calculated up to the 200th harmonic.

4.3. COMPARISON OF THE THD_{Ia} DEFINITIONS

This part of the paper compares the above-mentioned definition of the THD_{Ia}. Figures 18 and 19 present the dependence of the THD_{Ia} on the switching frequency for two dead times durations (t_d = 3 μs, t_d = 6 μs). It can be observed that the graphs can be divided into three parts. The first part I is up to the switching frequency around 2.25 kHz, the influence of the switching frequency dominates in this section. The third part III is from 6 kHz to 10 kHz, the effect of the dead time duration dominates in this section. The difference between the two definitions of the THD_{Ia} is negligible in these two sections I and III. The deviation between the formulations of the THD_{Ia} is obvious in the second section II which is from 2.2 kHz to 6 kHz. The both parameters – switching frequency and dead time duration – have the main effect on the THD_{Ia}.

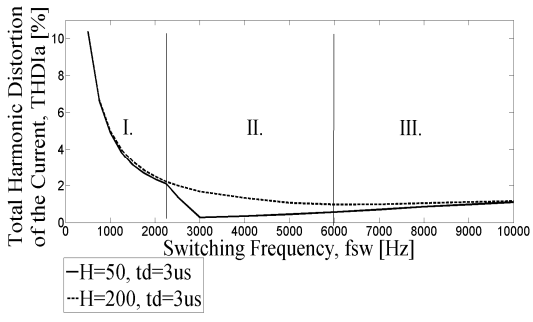

Fig. 18 – Comparison of the THD_{Ia} definitions; dead time is set to 3 μs.

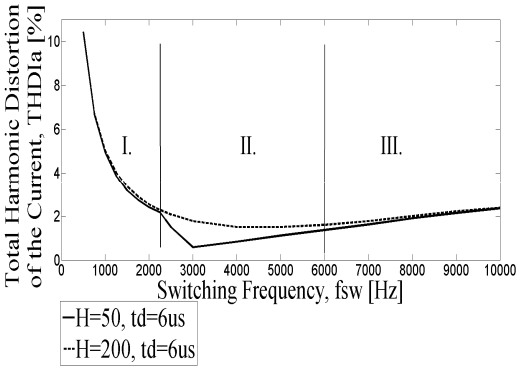

Fig. 19 – Comparison of the THD_{Ia} definitions; dead time is set to 6 μs.

5. **CONCLUSIONS**

The paper presents the study of the current harmonics drawn from the grid by voltage-source active rectifiers. The input current harmonics orders and values are derived. The equation (5) shows that input current harmonics are independent on the load of voltage-source active rectifiers. The main parameters that affect harmonics are the rectifier input voltage harmonics and the input impedance.

The next part proves that the above-mentioned equations apply even if the switching frequencies are random and non-integer multiples of the grid frequency.

The main section of the paper deals with the effect of the dead time duration. In accordance with the equation (3) and (9) and Fig. 10, it is obvious that dead times affect the characteristics harmonics; the characteristics harmonics appear in the input current spectrum. With regard to the low orders of characteristics harmonics, the characteristics harmonics values are not dangerous, even though the characteristics harmonics values can be higher than the harmonics satisfying the equation (2).

The last part discusses the calculation approach of the total harmonics distortion of the input current, if the switching frequencies are higher than 2.5 kHz. With regard to the conclusion of the Section 4 and Figs. 18 and 19, it is recommended that the total harmonic distortion of the input current should be calculated up to the harmonics order that are higher than the switching frequency. Furthermore, the influence of the dead times are proved.

The mentioned recommendation about calculation of the total harmonic distortion of the input current up to the high frequencies can be applied on all converters types that are switched by higher frequencies than 2.5 kHz. The calculations of the high input current harmonics orders are significant in the case of the grid resonance, where converters are connected; the small values of the input current harmonics can cause unacceptable voltage harmonics values of the grid.

ACKNOWLEDGEMENTS

This work was supported by the project Research and Development of Perspective Technologies in Electric Drives and Machines II SGS-2015-038.

Received on September 10, 2016

REFERENCES

1. S.R. Bowes, *New sinusoidal pulsewidth-modulated invertor*, Engineers Electrical, Proceedings of the Institution of, **122**, *1*, pp. 1279–1285 (1975).
2. S.R. Bowes, B.M. Bird, *Novel approach to the analysis and synthesis of modulation processes in power convertors*, Electrical Engineers, Proceedings of the Institution of, **122**, *5*, pp. 507–513 (1975).
3. B. Mokrytzki, *Pulse width modulated inverters for ac motor drives*, IEEE Transactions on Industry and General Applications, **IGA-3**, *6*, pp. 493–503 (1967).
4. J. Hamman, F.S. Van Der Merwe, *Voltage harmonics generated by voltage-fed inverters using PWM natural sampling*, IEEE Transactions on Power Electronics, **3**, *3*, pp. 297–302 (1988).
5. D.G. Holmes, T.A. Lipo, *Pulse width modulation for power converters: principles and practice*, John Wiley & Sons, 2003.
6. K.K. Tse, *et al*., *A comparative study of carrier-frequency modulation techniques for conducted EMI suppression in PWM converters*, IEEE Transactions on Industrial Electronics, **49**, *3*, pp. 618–627 (2002).
7. Y. Murai, T. Watanabe, H. Iwasaki, *Waveform distortion and correction circuit for PWM inverters with switching lag-times*, IEEE transactions on Industry Applications, **IA-23**, *5*, pp. 881–886 (1987).
8. C.M. Wu, W.H. Lau, H.S.H. Chung, *Analytical technique for calculating the output harmonics of an H-bridge inverter with dead time*, IEEE Transactions on Circuits and Systems I: Fundamental Theory and Applications, **46**, *5*, pp. 617–627 (1999).
9. F. Chierchie, E.E. Paolini, *Quasi-analytical spectrum of PWM signals with dead-time for multiple sinusoidal input*, Circuits and Systems (ISCAS), IEEE International Symposium on, 2011, pp. 1033–1036.
10. F. Chierchie, *et al*, *Frequency analysis of PWM inverters with dead-time for arbitrary modulating signals*, IEEE Transactions on Power Electronics, **29**, *6*, pp. 2850–2860, 2014.
11. A.M. Dumitrescu, *et al*., *Current controllers design using naslin polynomial method for active power filters*, Rev. Roum. Sci. Techn. – Électrotechn. et Énerg., **54**, *1*, pp. 115–124 (2009).
12. R. Abdollahi, *A novel tapped delta autotransformer based 72-pulse AC-dc converter with reduced kilovolt-ampere rating for power quality improvement*, Rev. Roum. Sci. Techn. – Électrotechn. et Énerg., **61**, *1*, pp. 173–177 (2016).
13. Z. Boudries, Adel Aberbour, K. Idjdarene, *Study on sliding modevirtual flux oriented control for three-phase PWM rectifiers*, Rev. Roum. Sci. Techn. – Électrotechn. et Énerg., **61**, *2*, pp. 153–158 (2016).
14. S.A. Tadjer, I. Habi, *Improvement of the quality of electrical power by a photovoltaic generator connected to the grid*, Rev. Roum. Sci. Techn. – Électrotechn. et Énerg., **61**, *1*, pp. 37–41 (2016).
15. L.E. Petrean, *et al*., *The effect of power quality disturbances on the electromagnetic compatibility*, Rev. Roum. Sci. Techn. – Électrotechn. et Énerg., **53**, pp. 147–154 (2008).
16. Y. Yang, *et al*., *Harmonics mitigation of dead time effects in PWM converters using a repetitive controller*, Applied Power Electronics Conference and Exposition (APEC), 2015, pp. 1479–1486.
17. D. Floricau, T. Tudorache, L. Kreindler, *New Boost-Type PFC MF-Vienna PWM Rectifiers with Multiplied Switching Frequency*, Advances in Electrical and Computer Engineering, **15**, *4*, pp. 81–86 (2015).
18. P.W. Lehn, *Direct harmonic analysis of the voltage source converter*, IEEE Transactions on Power Delivery, **18**, *3*, pp. 1034–1042 (2003).

19. V. Kus, Tereza Josefova, *The use of theory of frequency modulation for the calculation of current harmonics of the voltage-source active rectifier*, Applied Electronics (AE), International Conference on, 2013, pp. 1–4.
20. V. Kus, Tereza Josefova, *Current harmonics of voltage-source active rectifier with random switching frequency*, Electric Power Engineering (EPE), Proccedings of the 15th International Scientific Conference on, 2014, pp. 193–196.
21. V. Kus, P. Drabek, Tereza Josefova, *Education strategy regarding the electromagnetic compatibility at low-freqeuncy*, Rev. Roum. Sci. Techn. – Électrotechn. et Énerg., **61**, *1*, pp. 48–52 (2016).
22. IEC 60050-551-20, *International Electrotechnical Vocabulary, Power Electronics – Harmonics Analysis*, 2003.
23. Tereza Josefova, V. Kus, *Influence of a dead time duration on the input current spectrum of voltage-source active rectifiers*, Energy (IYCE), International Youth Conference on, 2015, pp. 1–6.
24. L. Ben-Brahim, *The analysis and compensation of dead-time effects in three phase PWM inverters*, *Industrial Electronics Society*, IECON '98. Proceedings of the 24th Annual Conference of the IEEE, 1998, pp. 792–797.
25. G. Grandi, J. Loncarski, R. Seebacher, *Effects of current ripple on dead-time distortion in three-phase voltage source inverters*, Energy Conference and Exhibition (ENERGYCON), 2012, pp. 207–212.
26. A.R. Munoz, T. Lipo, *On-line dead-time compensation technique for open-loop PWM-VSI drives*, IEEE Transactions on Power Electronic, **14**, *4*, pp. 683–689 (1999).
27. M. Herrán, *et al*., *Adaptive dead-time compensation for grid-connected PWM inverters of single-stage PV systems*, IEEE Transactions on Power Electronics, **28**, *6*, pp. 2816–2825 (2012).
28. D.C. Moore, M. Odavic, S.M. Cox, *Dead-time effects on the voltage spectrum of a PWM inverter*, IMA Journal of Applied Mathematics, **79**, *6*, pp. 1061–1076 (2014).